

1 **The *Aphelenchoides* genomes reveal major events of horizontal gene**  
2 **transfers in clade IV nematodes**

3

4 Cheng-Kuo Lai<sup>1,2</sup>, YiChien Lee<sup>1,3,4</sup>, Huei-Mien Ke<sup>1</sup>, Min R Lu<sup>1</sup>, Wei-An Liu<sup>1</sup>, Hsin-Han  
5 Lee<sup>1</sup>, Yu-Ching Liu<sup>1</sup>, Toyoshi Yoshiga<sup>5</sup>, Taisei Kikuchi<sup>6</sup>, Peichen J. Chen<sup>7\*</sup> and Isheng  
6 Jason Tsai<sup>1,2\*</sup>

7

8 Correspondence: [janetchen@nchu.edu.tw](mailto:janetchen@nchu.edu.tw) and [jjtsai@gate.sinica.edu.tw](mailto:jjtsai@gate.sinica.edu.tw)

9

10

11 <sup>1</sup>Biodiversity Research Center, Academia Sinica, Taipei 11529, Taiwan.

12 <sup>2</sup>Genome and Systems Biology Degree Program, National Taiwan University and  
13 Academia Sinica, Taipei, Taiwan.

14 <sup>3</sup>Biodiversity Program, Taiwan International Graduate Program, Academia Sinica and  
15 National Taiwan Normal University, Taipei, Taiwan

16 <sup>4</sup>Department of Life Science, National Taiwan Normal University, 116 Wenshan, Taipei,  
17 Taiwan

18 <sup>5</sup>Faculty of Agriculture, Saga University, Saga 840-8502 Japan

19 <sup>6</sup>Department of Integrated Biosciences, Graduate School of Frontier Sciences, The  
20 University of Tokyo, Chiba, 277-8562, Japan

21 <sup>7</sup>Department of Plant Pathology, National Chung Hsing University, Taichung, Taiwan

22

23

24

25

26

27

28

29

30

31

32 **Abstract**

33

34 *Aphelenchoides besseyi* is a plant-parasitic nematode (PPN) in the Aphelenchoididae  
35 family capable of infecting more than 200 plants. *A. besseyi* is also a species complex  
36 with strains exhibiting varying pathogenicity to plants. We present the genome and  
37 annotations of six *Aphelenchoides* species, four of which belonged to the *A. besseyi*  
38 species complex. Most *Aphelenchoides* have a genome size of 44.7-47.4 Mb and are  
39 amongst the smallest in the clade IV, with the exception of *A. fujianensis*, which has a  
40 size of 143.8 Mb and is the largest. Phylogenomic analysis successfully delimited the  
41 species complex into *A. oryzae* and *A. pseudobesseyi* and revealed a reduction of  
42 transposon elements in the last common ancestor of *Aphelenchoides*. Synteny analyses  
43 between reference genomes indicated that three chromosomes in *A. besseyi* were  
44 derived from fission and fusion events. A systematic identification of horizontal gene  
45 transfer (HGT) genes across 27 representative nematodes allowed us to identify two  
46 major episodes of acquisition corresponding to the last common ancestor of clade IV or  
47 major PPNs, respectively. These genes were mostly lost and differentially retained  
48 between clades or strains. Most HGT events were acquired from bacteria, followed by  
49 fungi, and also from plants which was especially prevalent in *Bursaphelenchus*  
50 *mucronatus*. Our results establish a comprehensive understanding on new origins of  
51 horizontal gene transfer in nematodes.

52

53

54

55

56

57

58

59

60

61

62

## 63 Introduction

64

65 The ability to parasitise plants has evolved in the phylum Nematoda on at least  
66 four occasions<sup>1,2</sup>. The major plant parasites belonged to the Aphelenchodidae and  
67 Parasitaphelenchidae families making up the Aphelenchoidea superfamily and the  
68 Tylenchida order of clade IV nematodes<sup>3</sup>; these plant parasitic nematodes (PPNs)  
69 collectively cause worldwide agriculture damages of over US\$80 billion each year<sup>4</sup>.  
70 Root-knot nematodes in *Meloidogyne* genus cause the majority of these losses and  
71 were the first of PPNs to have their genomes sequenced<sup>5</sup>, followed by pinewood  
72 nematode *Bursaphelenchus xylophilus*<sup>6,7</sup>, potato cyst nematode *Globodera pallida*<sup>8</sup>,  
73 soybean cyst nematode *Heterodera glycines*<sup>9</sup> and others<sup>10,11</sup>. Comparing these  
74 genomes yield insight into several adaptations that allow PPNs to parasitize plants.  
75 Examples include effectors such as carbohydrate active enzymes (CAZyme), which are  
76 known to be secreted by PPNs and are hypothesized to be involved in degrading or  
77 modifying the composition of different plant structural tissues<sup>12,13</sup>. Some of these PPN-  
78 specific genes are known to be acquired from bacteria or fungi through horizontal gene  
79 transfer (HGT)<sup>14</sup>, giving nematodes the ability to adapt to different environments<sup>14</sup>.  
80 Although numerous HGT genes have been identified and documented in different  
81 nematodes, research on the timing and subsequent maintenance of these genes, and  
82 why their copy numbers differ, has been restricted to a few PPN clades<sup>15</sup>.

83

84 Currently, the only major groups containing plant parasitic nematodes that lack a  
85 reference genome are Trichodoridae and Aphelenchoididae. Of particular interest is the  
86 *Aphelenchoides besseyi*, which is a foliar nematode that infects almost 200 plants in 35  
87 genera<sup>16</sup>. This nematode is 10mm in body size, has a life cycle of this nematode is  
88 around 10 to 12 days and it can reproduce in extreme environments, making it hard to  
89 eliminate. Better known as the rice white tip, *A. besseyi* infects important agronomic  
90 crops such as rice, soybeans and strawberries<sup>17,18</sup>, causing necrosis and distortion of its  
91 host's leaves<sup>16,18,19</sup>. The nematode has reportedly been responsible for up to a 60%  
92 crop loss in some cases<sup>20,21</sup> and was listed among the top ten plant parasitic  
93 nematodes in a recent review<sup>22</sup>. Despite the economic damage these parasitic

94 nematodes inflict, particularly in the Asian region, little is known about the basic biology,  
95 genetic diversity or evolution of *A. besseyi* and other Aphelenchoididae members. It has  
96 been reported that *A. besseyi* isolated from different hosts have different levels of  
97 pathogenicity. For instance, the populations of *A. besseyi* isolated from strawberries  
98 were unable to parasitise rice<sup>21</sup>. However, the populations of this species from bird's-  
99 nest fern can reproduce in both rice and strawberries<sup>19</sup>. Despite their almost overlapping  
100 morphological features, we previously identified copy number variations of genes  
101 encoding cell-wall-degrading enzymes including glycosyl hydrolase family 5 (GH5) and  
102 GH45 cellulases between *A. besseyi* of different host origins<sup>23</sup>. An 18S phylogeny  
103 separated the strains isolated from rice and fern unambiguously, suggesting that *A.*  
104 *besseyi* might be a species complex, with literatures also identifying variations in  
105 different molecular markers in different hosts that are original to *A. besseyi*<sup>18,24</sup>.  
106 Subbotin *et al.* recently used a combination of molecule makers (28S, ITS and  
107 mitochondria *COI* gene)<sup>17</sup> to reclassify foliar nematodes into three separated clades: the  
108 *A. besseyi* isolated mainly from strawberries, the *A. oryzae* mainly isolated from rice and  
109 *A. pseudobesseyi* from wood fern suggesting this species complex may be well  
110 differentiated at the genome level. From an evolutionary perspective, *A. besseyi* is also  
111 interesting because its primitive plant parasitism was a relatively recent evolutionary  
112 adaptation<sup>25</sup>.

113  
114 In this study, we sequenced and annotated the genomes of four *A. besseyi*  
115 species complex strains isolated from different plants which we later designated as *A.*  
116 *pseudobesseyi* and *A. oryzae*, and another two species in the Aphelenchoididae family  
117 (*Aphelenchoides bicaudatus* and *Aphelenchoides fujianensis*). We compared the  
118 proteomes of six Aphelenchoididae members with 21 other representative nematodes to  
119 delimit species relationships and investigated their gene family dynamics. We identified  
120 synteny with representative nematodes and inferred rearrangement events to determine  
121 how the three chromosomes of *A. besseyi* was evolved. The availability of the  
122 *Aphelenchoides* assemblies allowed us to systematically determine the horizontal gene  
123 transfer-acquired genes in nematode genomes. By inferring the evolutionary origins of  
124 these HGT genes we found historical HGT events that shaped nematode evolution.

125 The major event occurred in the last common ancestor of clade IV nematodes and may  
126 have contributed to the early adaptation of these nematodes.

127  
128

## 129 **Results**

130

### 131 **Genome assemblies and annotations of six *Aphelenchoides* species**

132 We sequenced and assembled the genomes of six nematodes in the  
133 *Aphelenchoides* genus (four *A. besseyi*, one *A. bicaudatus* and one *A. fujianensis*).  
134 These species were chosen to represent the Aphelenchoididae family and *A. besseyi*  
135 strains isolated from three plant hosts (**supplementary table S1**) to delimit their  
136 relationship within the species complex. For each species, an initial assembly was  
137 produced from either 70-148X Oxford Nanopore or 113-422X Pacbio reads using Flye  
138 assembler<sup>26</sup> and further polished using Illumina reads (**supplementary table S2**).  
139 Among *A. besseyi* assemblies, the VT strain isolated from tape grass *Vallisneria spiralis*  
140 had the highest genome quality with N50 5.4 Mb (hereafter denoted as APVT). The  
141 contigs of this strain were further scaffolded with 150X Hi-C reads using the Juicer  
142 program<sup>27</sup> (**supplementary fig. S1**) yielding a final assembly of 44.7 Mb (N50 = 16.9  
143 Mb). More than 99% of this assembly was in three scaffolds, presumably corresponding  
144 to three chromosomes<sup>28</sup> (2n=6). Five *Aphelenchoides* assemblies ranged from 44.7 to  
145 47.4 Mb (N50 = 12.2-17.8 Mb; **supplementary table S3**), and a sixth assembly (*A.*  
146 *fujianensis*) of 143.8 Mb (N50 = 553 kb; **supplementary table S3**) was estimated to be  
147 triploid<sup>29</sup> (**and supplementary fig. S2**). Although not present in the assemblies, the  
148 telomere motif TTAGGC was identified in the reads of *A. pseudobesseyi* at low  
149 coverage (**Supplementary Info**), which is consistent to the sister group species of *B.*  
150 *xylophilus* (**supplementary table S4**) indicating the presence of telomeres in these  
151 species.

152 Using the proteomes of *Bursaphelenchus xylophilus* and *Caenorhabditis*  
153 *elegans*, and the transcriptomes of pooled worms in each species as evidences, we  
154 predicted 11,701 to 12,948 protein coding genes in six *Aphelenchoides* species with  
155 Maker2 pipeline<sup>30</sup> (**supplementary table S3**). With the exception of *A. fujianensis*,  
156 these were fewer protein coding genes in these species than in Tylenchida nematodes

157 (12,762 to 19,212) and free-living nematodes (20,184 to 20,992). The completeness of  
158 annotated genes was estimated to be 76.4–81.3% based on a BUSCO assessment,  
159 lower than that of *Bursaphelenchus* species (83.0–89.4%), but are higher than that of  
160 Tylenchida (59.8–73.8%) nematodes. The lower BUSCO completeness in  
161 *Aphelenchoidea* was likely clade specific as re-annotation of the APVT strain with  
162 trained models based on manual curation of 975 genes also gave a similar score of  
163 78.2%. Among them, 66.5% to 71.0% of genes in *Aphelenchoidea* could be assigned at  
164 least a domain from the Protein family (Pfam) database<sup>31</sup>. In addition, orthologous  
165 groups were inferred with the proteomes of six *Aphelenchoidea* with 21 other  
166 nematodes using Orthofinder<sup>32</sup>. With the exception of *A. fujianensis*, 78.5–85.4% (*A.*  
167 *fujianensis* = 48.7%), 69.4–76.9% (*A. fujianensis* = 42.8%) and 87.5–98.7% of  
168 *Aphelenchoidea* genes were orthologous to *B. xylophilus*, *C. elegans* and at least one  
169 other nematode species, respectively, suggesting that the reduced proteome in most  
170 *Aphelenchoidea* was mainly comprised of conserved genes among nematodes.

171

### 172 **Phylogenomics delimit species complex of *Aphelenchoidea besseyi***

173 To investigate the evolution of plant-parasitic nematodes and the relationships  
174 among members in the *A. besseyi* species complex, a maximum-likelihood phylogenetic  
175 tree was constructed based on 74 low-copy orthologues. The phylogeny is consistent  
176 with a the previous study<sup>33</sup>: the major plant parasitic nematodes were divided into  
177 Aphelenchoidea and Tylenchida, and six *Aphelenchoidea* species were grouped as  
178 sister to *Bursaphelenchus* (**fig. 1a**). The *A. besseyi* strains were clustered into two  
179 groups based on their hosts, suggesting that relationships in these species within the *A.*  
180 *besseyi* species complex can be unambiguously resolved based on their different  
181 lifestyles and host preferences. Combined with the previous 28S phylogeny of the *A.*  
182 *besseyi* species complex<sup>17</sup> (**supplementary fig. S3**), we further designated these two  
183 groups as *A. oryzae* and *A. pseudobesseyi* groups isolated from rice or other plants  
184 (land grass and bird's-nest fern). The median nucleotide and amino acid identity was  
185 86.6% and 90% between these two groups, respectively (**supplementary fig. S4**).  
186 Strains in each group also differed in heterozygosity (0.017-0.019% in *A. oryzae* vs  
187 0.071-0.075% in *A. pseudobesseyi*) and changes in recent effective population sizes

188 inferred using pairwise sequentially Markovian coalescent (PSMC) analysis<sup>34</sup>  
189 (**supplementary fig. 5**). Together these results emphasised that relationships among  
190 species in the *A. besseyi* species complex were highly diversified at the genome level  
191 despite being challenging to differentiate based solely on morphology<sup>17</sup>.

192

### 193 **Genome reduction as a result of transposable element loss**

194 The *Aphelenchoides* genomes were smaller than those of other plant-parasitic  
195 nematodes (**fig. 1b** and **supplementary table S3**), indicating that genome reduction  
196 took place in the last common ancestor of the *Aphelenchoides* genus. Much of the  
197 reduction can be explained by the reduced markup of repeat content compared to other  
198 nematodes (**fig. 1b**). The dominant transposable elements of *Aphelenchoides* were  
199 DNA transposons—which were reduced in content (0.14–1.36 Mb vs. 4.2–22.1 Mb)—  
200 and number of families (1–7 in *Aphelenchoides* compared to 9 and 26 in *B. xylophilus*  
201 and *H. glycines*, respectively) compared to other nematodes. Fewer LTR (0.07–0.8 Mb  
202 vs. 0.24–9.3 Mb) and LINE (0.0006–0.66 Mb vs 0.02–4.5 Mb) retrotransposons were  
203 also observed in this genus. These results suggest that the reduced genome sizes in  
204 *Aphelenchoides* might have been caused by the rapid loss of transposable elements  
205 and led to the eventual loss of entire families in some cases (**fig. 2a**). Within the *A.*  
206 *besseyi* species complex, *A. pseudobesseyi* contained significantly fewer DNA  
207 transposons, LTR and LINE retrotransposons than *A. oryzae* (**fig. 2a and**  
208 **supplementary fig. 6**).

209

210

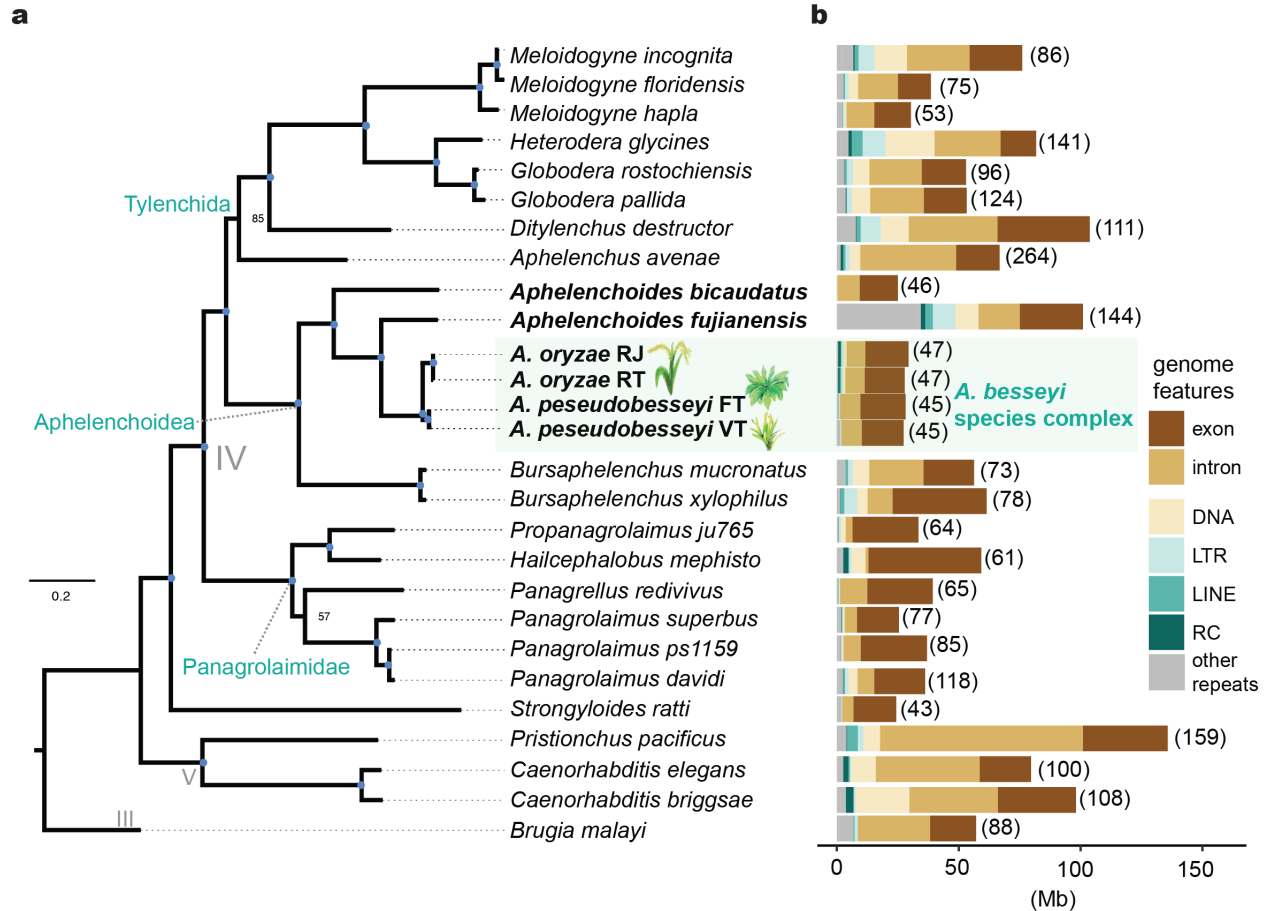
211

212

213

214

215



216

217 **Figure 1 Phylogenomic analysis of plant-parasitic nematodes.** **a.** The phylogeny of 27  
 218 representative nematodes was inferred based on the concatenation of protein sequences from  
 219 74 low-copy orthologues. The blue dots in branches denote a bootstrap value of 100. **b.** The  
 220 size of the genome features in nematodes, repeats containing DNA transposons (DNA), long  
 221 interspersed nuclear elements (LINE), long terminal repeats (LTR), rolling-circular (RC) and the  
 222 unclassified repeats are labelled as “other repeats”. Numbers in brackets denote genome  
 223 assembly sizes in megabases.

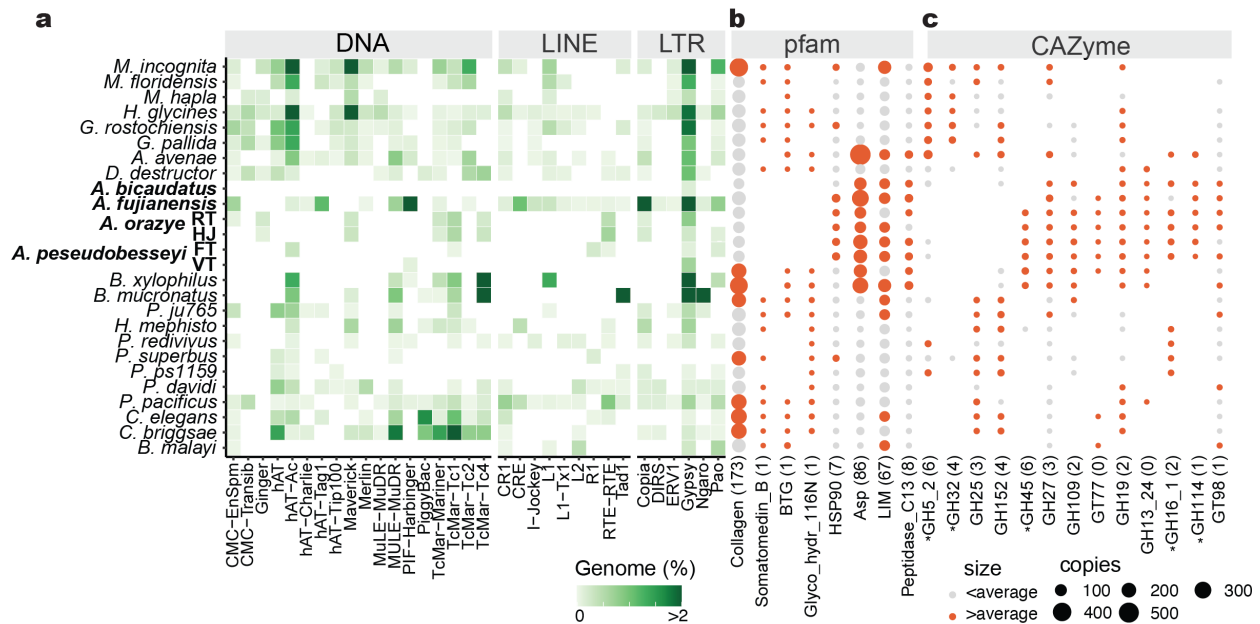
224

225

226



227



228

229 **Figure 2 Repeat and proteome contents in nematodes.** **a.** The genome proportions of DNA,  
 230 LINE and LTR transposable elements in nematodes shown by genome percentage **b-c.** Protein  
 231 families and CAZyme gene copy numbers vary significantly among nematodes. The dot size  
 232 represents the copy number of each domain and the different colour represents the copy  
 233 number of domains larger or lower than average copies shown in brackets.

234

235

### 236 Gene family specialization in the *Aphelenchoides* species

237 We observed 66 enriched and 31 reduced protein domains in the four member of  
 238 the *A. besseyi* species complex compared to 21 other nematodes. (**fig. 2b** and  
 239 **supplementary table S5**). Domain reduction included collagen (90–109 copies in the  
 240 *A. besseyi* species complex vs. 72–407 in others), Somatomedin B and BTG. Genes  
 241 containing collagen domains were reportedly associated with capsule formation; the  
 242 reduced copy of collagen domains in *Trichinella spiralis* were thought to contribute its  
 243 lower host-specificity than other nematodes<sup>35</sup>, and may be related to the wide host  
 244 range of *A. besseyi*. In contrast, Aphelenchoidea members possess on average four-  
 245 fold (91–314 vs. 4–555 copies) more aspartic proteases (ASP) than other nematodes  
 246 (**supplementary table S5**). ASPs were reported to associate with the digestion of host  
 247 haemoglobin in *Haemonchus contortus*<sup>36</sup>, and also skin penetration in hookworms<sup>37</sup>,

248 and may play an important role in the *Aphelenchoides*'s parasitism process. Other  
249 expansions included LIM and peptidase C13 domains, which participate in participating  
250 in the regulation of cell motility and cell growth<sup>38</sup> or degradation of protein tissues in a  
251 host<sup>39</sup>, emphasizing that these domain dynamics are associated with adaptations to  
252 plant parasitism.

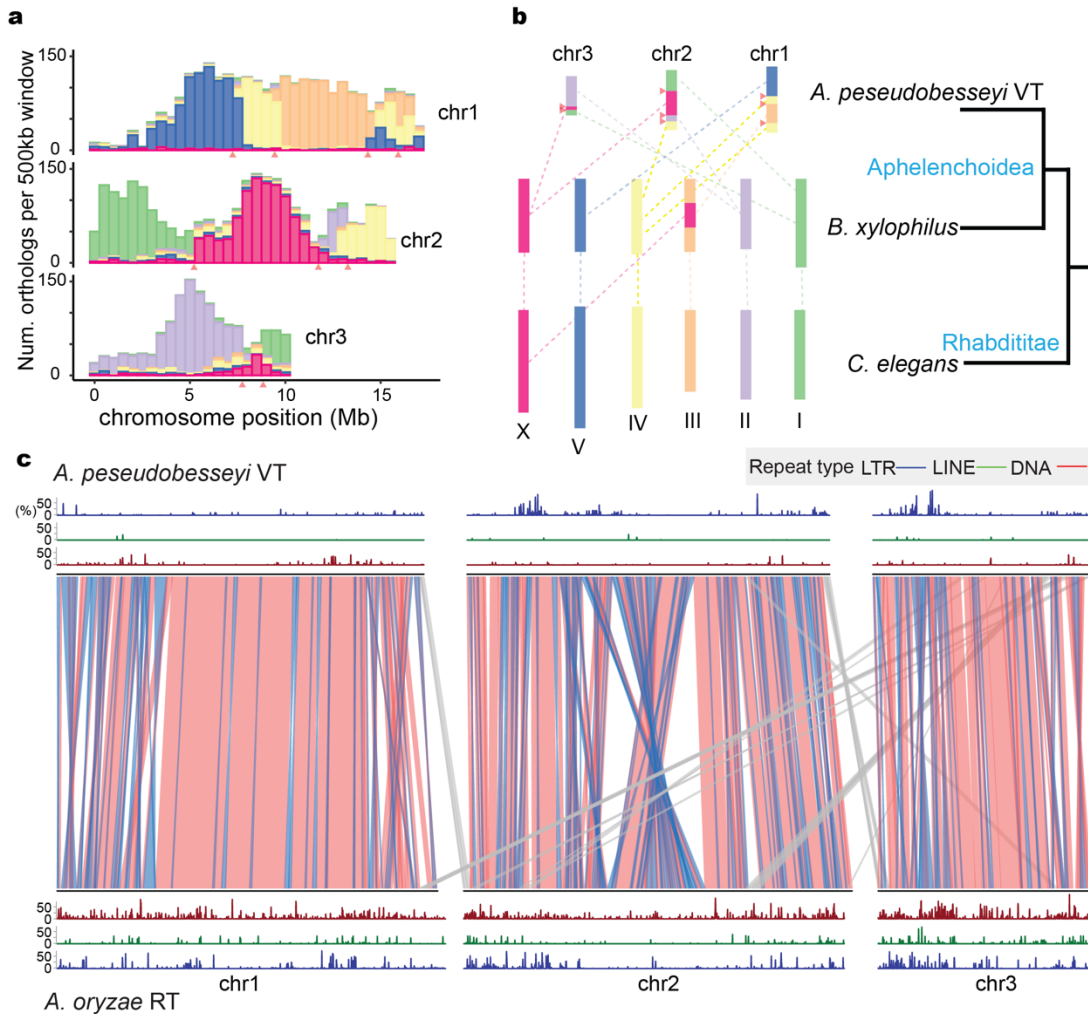
253 The plant cell wall acts as a primary defensive barrier and the production of  
254 carbohydrate-active enzyme (CAZyme) families are important for PPNs to infect plants.  
255 A total of 132 CAZyme families were identified in the representative the 27 nematodes.  
256 Of these, 59–67% of the CAZyme families were observed in Aphelenchoidea which is  
257 similar to the 55–66% and 58–68% of the families in Tylenchida and free-living  
258 nematodes (**supplementary table S6**), respectively. A total of 13 families were  
259 significantly expanded or lost in the *Aphelenchoides* genus (**fig. 2c**), including GH16,  
260 GH27 and GH45. GH16 serves as the putative  $\beta$ -glycanases involved in the  
261 degradation or remodelling of cell wall polysaccharides<sup>40</sup>, GH16 had one to six copies in  
262 Aphelenchoididae nematodes and was not identified outside this clade except in *D.*  
263 *destructor*, in which there were three copies. There are three to 11 copies of GH27—  
264 which are reportedly involved in the function of hemicellulose and associated with  $\alpha$ -  
265 galactosidase activity in both bacteria and fungi<sup>41</sup>— in Aphelenchoidea, but fewer in the  
266 Tylenchida nematodes. The previously identified GH45 present in Aphelenchoidea  
267 nematodes<sup>23</sup>—involved in the degradation of beta-1,4-glucans in the plant cell wall<sup>19</sup>—  
268 possess different copy numbers between *A. pseudobesseyi* and *A. oryzae* and were  
269 absent in *A. fujianensis* and *A. bicaudatus*, suggesting differential maintenance of these  
270 genes in the same genus may have contributed to variations of pathogenicity to plants.

271

## 272 **Chromosome evolution of PPNs**

273 To investigate the extent of the karyotype rearrangements in *Aphelenchoides*, we  
274 inferred the synteny relationships among *A. pseudobesseyi* (chromosome n=3)<sup>28</sup>, *B.*  
275 *xylophilus* (n=6) and *C. elegans* (n=6) using single copy orthologs. Within the three *A.*  
276 *pseudobesseyi* chromosomes, orthologs belonging to all *C. elegans* chromosomes  
277 were clustered into distinctive blocks (**fig. 3a**) suggesting a fusion of ancestral  
278 chromosomes. These regions remained contiguous and contained 148–801 orthologous

279 genes that could be assigned from individual chromosomes presumably not yet broken  
280 down yet by recombination, allowing us to pinpoint the fusion points and infer the order  
281 of rearrangement events based the constitution of chromosomes (**fig. 3b**). We  
282 encountered instances of where an ancestral chromosome was found in different parts  
283 of the *A. pseudobesseyi* chromosomes, suggesting fission also took place. In the case  
284 of chr IV—which remained homologous in *C. elegans* and *B. xylophilus*—corresponding  
285 synteny blocks in *A. pseudobesseyi* were identified in the arm of chr 2 and chr 1  
286 separated by regions of chr III origin (**fig. 3b**). The majority of the ancestral sex  
287 chromosomes were unambiguously assigned to chr 2, and remapping of male  
288 sequences showed equal coverage along the chromosomes (**supplementary figure**  
289 **S7**), suggesting that the Aphelenchoidea superfamily including *A. besseyi* exhibited a  
290 stochastic sex determination system that was recently characterized in *B. xylophilus*<sup>42</sup>.  
291 Within the *A. besseyi* species complex, a total of 91% and 88% of genomes were in  
292 synteny between APVT and AORT, respectively. Intra-chromosomal inversions were  
293 common at chromosome arms. In addition, we identified a major inversion of length 3.4  
294 Mb long located in the centre of chr 2 (**fig. 3c**) suggesting rearrangement is still  
295 ongoing. Both the LTR and LINE retrotransposons were enriched in the chromosome  
296 arms of the *A. oryzae* strain (AORT) (**fig. 3c and supplementary fig. S6**), which is  
297 consistent with the hallmark of nematode chromosome evolution<sup>43</sup>. In contrast, only the  
298 LTR retrotransposons were found in the two chromosome arms of *A. pseudobesseyi*,  
299 suggesting that these repeats were differentially maintained after speciation.  
300



301  
 302 **Figure 3. Chromosome evolution of plant-parasitic nematodes.** **a.** The density of pairwise  
 303 single-copy orthologs between *A. pseudobesseyi* VT and *B. xylophilus*. Colours denote *B.*  
 304 *xylophilus* chromosomes and the putative chromosome fusion sites in APVT are labelled with  
 305 red triangles. **b.** Colours denote corresponding *C. elegans* chromosomes, and dashed lines  
 306 indicate linkage groups corresponding to ancestral chromosomes. **c.** The synteny relationship  
 307 and the distribution of transposable between *A. pseudobesseyi* VT and *A. oryzae* RT. Blocks  
 308 indicate synteny links between the two strains, and the line colours correspond to inversion  
 309 (blue) and inter-chromosomal rearrangement (grey). Distribution of DNA transposons (red), long  
 310 interspersed elements (green) and long terminal repeats (blue) between two stains are shown.

311  
 312  
 313  
 314  
 315

316 **Major episode of HGT in clade IV nematodes**

317 In plant parasitic nematodes, the GH5 cellulase was found present in Tylenchida  
318 and only *A. pseudobesseyi* and *A. bicaudatus* within the Aphelenchoidea clade<sup>23,44</sup>,  
319 raising the possibility that many of the horizontal gene transferred genes were acquired  
320 in the last common ancestor of major PPNs but were differentially lost. To identify such  
321 events, a total of 27 proteomes from representative nematodes including the  
322 *Aphelenchoides* genomes were searched for evidence of HGT by calculating the Alien  
323 Index (AI) score using Alieness<sup>45</sup>. We identified a total of 1,675 HGT orthogroups in 21  
324 nematodes. Placing these orthologs designated as events onto the species phylogeny  
325 assuming a parsimonious scenario<sup>46</sup>, indicated that HGT started in the last common  
326 ancestor of clade IV nematodes (**fig 4a**). Examples include GH16, GH32, GH43 and the  
327 aforementioned GH5 cellulases. We inferred a total of 161 orthogroups were acquired in  
328 this episode, and most of their origins were inferred to be bacteria (78.3%)  
329 (**supplementary table S7**) belonging to different genera, suggesting multiple  
330 acquisitions took place. Of these, we found 36 Pfam terms such as ABC transporter that  
331 were identified in multiple orthogroups suggesting some convergence in the acquired  
332 functions (**supplementary table S8**).

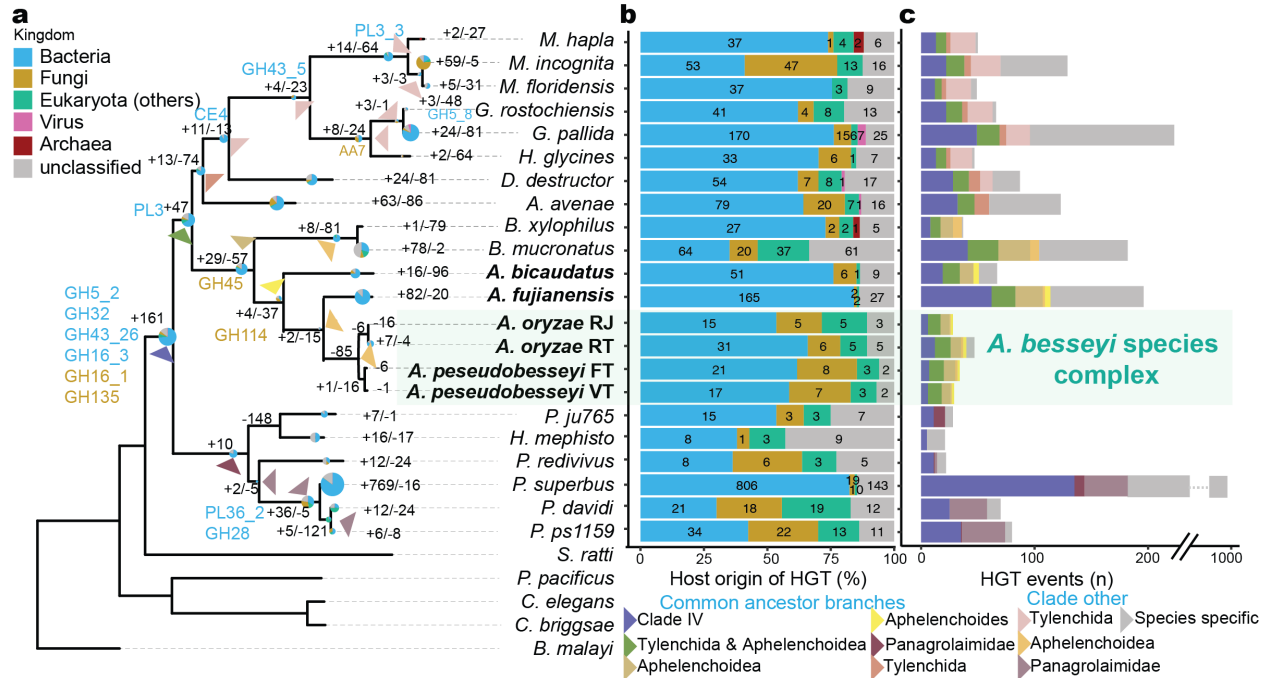
333 The revised GH5 cellulase phylogeny indicated an ancient duplication took place  
334 before the divergence of PPNs (**fig 5a**). One clade contains orthologs of the three  
335 *Panagrolaimid* (*P. sp.* PS1159, *P. superbus* and *P. davidi*), and Tylenchida, and the  
336 other clade contains members of Aphelenchoidea and Tylenchida nematodes, which  
337 emphasises that the fate of the HGT genes was governed by duplications and loss.  
338 Interestingly, the closest GH5 bacterial orthologs were *Salinimicrobium xinjiangense*  
339 and *Leeuwenhoekiella sp.*, which belonged to Flavobacteriaceae family and were from  
340 marine environments. We observed two GH16 subfamilies in nematodes. GH16\_3 in  
341 Tylenchida and *Bursaphelenchida* nematodes were clustered with bacterial origin  
342 sequences, whereas GH16\_1 of *Aphelenchoides* and *Panagrolaimus* nematodes were  
343 clustered with fungal origin (**fig 5b**), suggesting that the two GH16 groups arose  
344 independently. GH32 in *G. pallida*<sup>13</sup> is believed to play a role in the function of fructose  
345 hydrolysis and was found in one *Panagrolaimus* in addition to several Tylenchida  
346 nematodes (**supplementary fig. S8**). GH43 was identified at two distinct clusters of

347 bacterial origin in Tylenchida and *Panagrolaimid* nematodes which have been proposed  
348 to be involved in degradation of the hemicellulose in plants<sup>47</sup> (**supplementary fig. S9**).

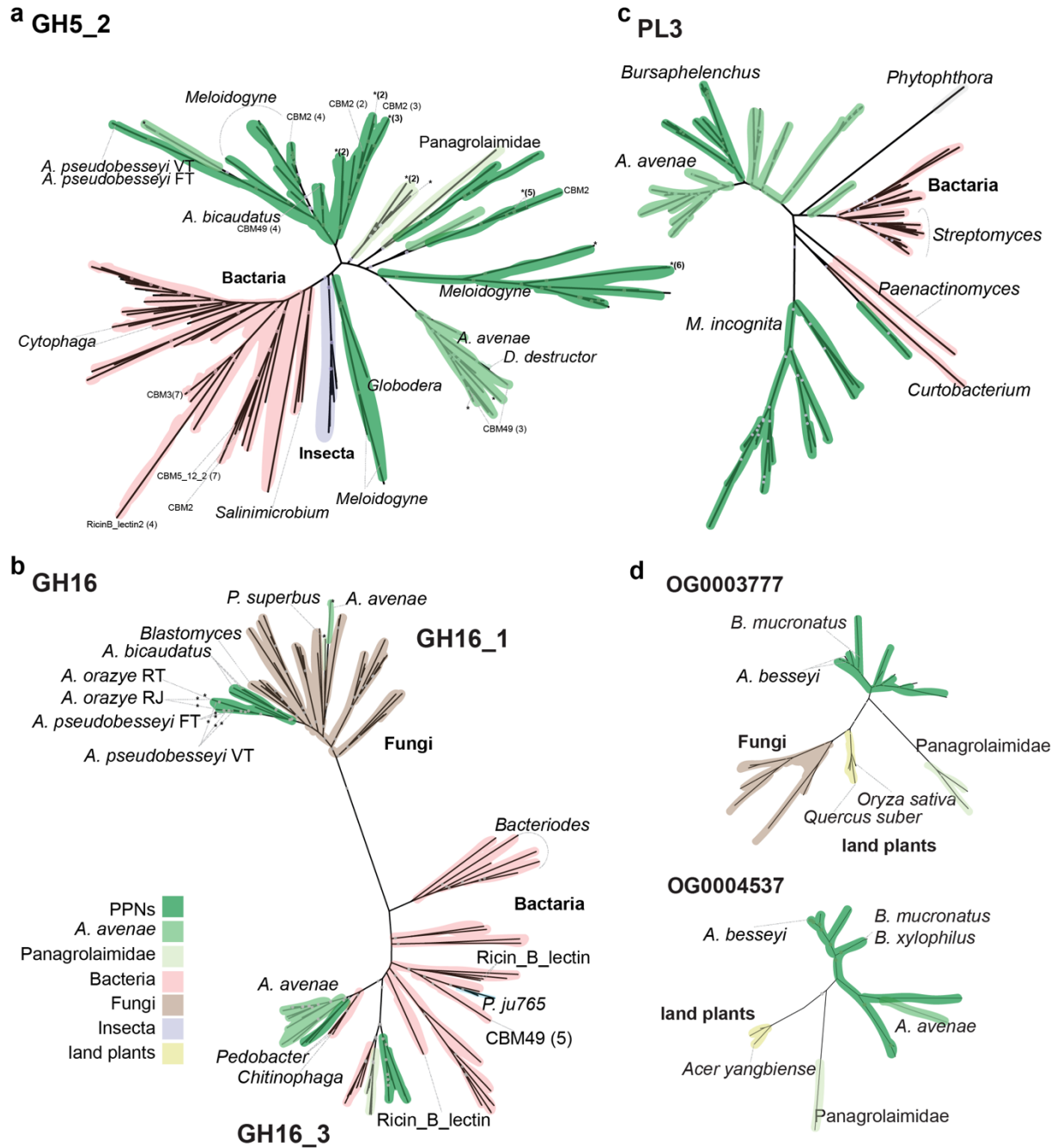
349 The next major episode of acquisition took place in the common ancestor of  
350 PPNs, with 47 orthogroups (**fig. 4a**). These families included pectate lyases 3 (PL3)  
351 which is associated with cell wall degradation<sup>48</sup>. The orthologs of PL3 in *Aphelenchus*  
352 *avenae* and two *Bursaphelenchus* nematodes were grouped together with distinct  
353 clusters of *Meloidogyne* species (**fig. 5c**) is consistent with previous phylogeny finding  
354 in PPNs<sup>44</sup>. The closest bacterial ortholog in the *Meloidogyne* clade was from  
355 *Curtobacterium flaccmfaciens* which is also known to cause bacterial wilt in the  
356 Fabaceae family<sup>49</sup>. Together, these results suggested some genes that were thought to  
357 play important roles in plant parasitism were in fact acquired earlier than the common  
358 ancestor of plant parasitic nematodes.

359 The majority of HGT gene families were of bacterial followed by fungal origin (**fig**  
360 **4b**). We also identified genes that were acquired from non-bacterial donors in the last  
361 common ancestors of clade IV, as well as in more recent, different PPN lineages (**fig**  
362 **4a**). This included the previously characterised fungal origin of GH45<sup>23,50</sup>, This cellulase  
363 family is present in most Aphelenchoidea nematodes except *A. fujinensis* and *A.*  
364 *bicaudatus*. The GH16 family was independently acquired from a bacterial and fungal  
365 donor in the last common ancestor of clade IV nematodes and the *Aphelenchoides*  
366 genus, respectively (**fig 5b**). Notably, we identified 40 orthogroups among PPNs that  
367 were transferred from the plant phylum Streptophyta, which is consistent with the finding  
368 of several sequences that are highly similar to plants in *H. glycine*<sup>51</sup> (**fig. 4b**). The  
369 closest plant orthologs included rice, maple and oak (**fig. 5d**) which are common hosts  
370 to many PPNs. Strikingly, of these orthogroups, 27 were present in *B. mucronatus* and  
371 enriched in the detoxification of cadmium and copper ion function (**supplementary**  
372 **table S9**), suggesting these genes may help *Bursaphelenchus* nematodes to degrade  
373 the toxin in pine wood hosts.

374



375  
 376 **Figure 4 The evolution of genes acquired from horizontal gene transfer (HGT) in clade IV**  
 377 **nematodes. a.** HGT orthogroups were inferred by the AI score<sup>52</sup> > 0 across 27 representative  
 378 nematodes; the HGT families gained or lost are shown in the branches. Horizontally acquired  
 379 CAZymes are annotated. The proportions of donor origins in each HGT orthogroup belonging to  
 380 different kingdoms of donors are shown as pie charts. The size of the pie chart corresponds to  
 381 the total number of HGT orthologues in branches; the chart was normalized using: log<sub>5</sub>(total  
 382 number). **b.** The distribution of HGT families transferred from different kingdoms, with the same  
 383 denoted color scheme as same as figure a. **c.** Number of HGT events among different inferred  
 384 time points corresponding with the branches which are triangle marked in the phylogeny.  
 385



386

387 **Figure 5 Phylogenies of nematode HGT orthogroups and their donor origin. a. GH5\_2 b.**

388 GH16 c. PL3 d. OG0003777 and OG0004537. Different colours denote different kingdoms and

389 species as shown in legend. Nematode gene copies with negative AI values were marked with

390 an asterisk. Additional Pfam domains are labelled when available. Nodes with iqtree UFBot

391 and SH-aLRT bootstrap support > 80% are labelled as grey circles.



392 We identified 0.3-2.4%, 0.6-2.1% and 0.1-5.4% proteomes among  
393 Aphelenchoidea, Tylenchida and *Panagrolaimomorpha* nematodes that were predicted  
394 to be HGT (**fig. 4c**). The majority of these differences were the result of clade-specific  
395 evolution after speciation. The high copy number of HGT genes observed in *M.*  
396 *incognita* was a result of duplication<sup>53</sup>, indicated by the fact that the number of HGT  
397 orthologs of bacteria origin were over two times higher than any other species  
398 (**supplementary fig. S10**). The high number of HGT genes in *P. superbus* was  
399 consistent with a previous study<sup>54</sup> and likely to be species specific.

400 To independently assess the accuracy of our approach and interrogate the fate  
401 of HGT genes, we constructed a phylogeny for every orthogroup containing identified  
402 HGT candidates. Members of Aphelenchoididae and Tylenchida orthologs in the  
403 majority of these orthogroups were predicted to be all HGT genes (with AI > 0; 54.6-  
404 76.5% vs. 77.3-89.4%). Genes from a species were typically grouped together in the  
405 orthogroup phylogeny regardless of being identified as HGT candidates, suggesting the  
406 genes that were not detected using our threshold shared common ancestries with those  
407 that were. Presumably, this was a result of accumulating substitutions over time.  
408 Consistent with this observation, the more ancient acquired HGT orthogroups in PPNs  
409 contained higher copy number of these genes compared to recently acquired families  
410 (**supplementary fig. S11**). The instances included GH5 families with 12.5-70.6% of  
411 copies in Tylenchida were failed to identify as HGT candidates, suggesting duplication  
412 and possibly neo-functionalisation of the GH family in PPNs after being acquired from  
413 bacterial origin (**fig. 5a**). The differentiation was ongoing and observed in the *A. besseyi*  
414 species complex, which included the GH45 orthogroup with negative AI in two *A. oryzae*  
415 strains (**supplementary fig. S12**).

416

## 417 Discussion

418 Characterising the diversity and comparing the genomes of plant parasitic  
419 nematodes has been of fundamental importance in understanding how such lifestyles  
420 arise and of practical importance in identifying candidate effectors and control methods.  
421 The latter has been addressed in several studies, focusing mainly on *Meloidogyne*<sup>55</sup>.  
422 The *Aphelenchoides* genome assemblies presented in this study allowed us to gain a

423 holistic view of the evolution of clade IV nematodes, which appeared to gain and lose  
424 many adaptations, including plant parasitism<sup>56</sup>. In their evolution, HGT genes have  
425 played important roles in functions related to these adaptations. The most recent  
426 comprehensive analyses of HGT in nematodes focused on plant parasitic nematodes<sup>15</sup>  
427 and found many of these genes were PPN specific. Of these, donors of gene families  
428 involved in plant cell-wall modifications were previously found to be associated with  
429 plants which was appealing that were sympatric with plant parasitic nematodes which  
430 made HGT possible<sup>44</sup>. Additional HGT events were identified in other clade IV  
431 nematodes<sup>13,54,57-59</sup> but were part of analysing new *de novo* genomes.

432 Our systematic investigation of HGT has instead shown that many of the  
433 aforementioned families were acquired much earlier in the last common ancestor of  
434 clade IV. Many clade IV nematodes are known to survive extreme desiccation<sup>54,59,60</sup> and  
435 the acquired HGT genes may be central to their resistance in harsh environment and  
436 subsequently catalysis to successful plant parasitism<sup>61</sup>. Sources of these donors may  
437 be the symbionts like the case of insects<sup>62</sup>, but currently nematode endosymbionts are  
438 restricted to *Wolbachia* and *Cardinium*<sup>63</sup> and were not identified in our analyses.  
439 Interestingly, many of the closest bacterial donors were from marine environments,  
440 raising the possibility that the last common ancestor of clade IV may have lived in a  
441 marine environment that underwent habitat transition<sup>64</sup>. However, we also identified  
442 donors of non-bacterial origin that were usually found in the environments that fit  
443 nematodes' present day lifestyle. Now that more genome sequences are available,  
444 historical HGT events were detected in the most recent common ancestor of major  
445 organism groups such as land plants<sup>65</sup>, of moths and butterflies<sup>66</sup>, which contributed  
446 the hosts' developmental roles and adaptations. These acquisitions were found to be  
447 episodic and likely took place in a time when either the host development or genome  
448 defence was vulnerable. We speculate that the gain and absence of gene families in  
449 clade IV nematodes may have played a role in retention of HGT genes.

450 The successful delimitation of the *A. besseyi* species complex unambiguously  
451 into *A. oryzae* and the recently proposed *A. pseudobesseyi* has important implications  
452 in nematode management. Congruent delimitation was observed between genomes  
453 and 28S phylogenies confirming the utility of species identification with existing

454 molecular markers<sup>18</sup>. *A. besseyi* is generally believed to have limited mobility in natural  
455 habitats, so its lack of population structure in China<sup>24</sup> was suggested as a consequence  
456 of human-mediated dispersal. Our results also supported that *A. oryzae* appears to be  
457 more rice plant specific compared to *A. pseudobesseyi* which was isolated more  
458 frequently in ornamental plants and other agronomic crops<sup>18</sup>. A comprehensive  
459 collection across a wider geographical range and resequencing of strains previously  
460 designated as *A. besseyi* could confirm whether *A. oryzae* was responsible for all the  
461 white tip disease in rice plants and may lead to better characterisations of the  
462 biogeography and evolution of different cryptic species.

463 The reduction of genome size and reduced chromosome numbers of *A. besseyi*  
464 represent an interesting outcome for the typical six nematode ancestral chromosomes  
465 around hundred megabases in length. Genome rearrangement and reduction are  
466 common across the tree of life including plants<sup>67</sup>, butterflies<sup>68</sup> and nematodes<sup>69</sup>. We  
467 show that *A. besseyi* underwent multiple chromosome fission and fusion events, and a  
468 possible explanation together with genome reduction may be the missing of meiosis  
469 genes and the telomeric repeat maintenance genes, which resulted in truncated meiosis  
470 (**supplementary table S10**); this was observed in an extreme case of *Diploscapter*  
471 *pachys*<sup>70</sup> possessing a single chromosome. Alterations in meiosis may lead to genome  
472 shrinkage due to a loss of transposable elements as a result of imbalanced chromatin  
473 as observed in *Caenorhabditis nigoni*<sup>71</sup>. It is likely that *Aphelenchoides* underwent a  
474 similar scenario. However, members of *Bursaphelenchus* with six chromosomes also  
475 failed to identify these aforementioned orthologs (**supplementary table S10**),  
476 suggesting their divergence has taken place since the last common ancestor of  
477 Aphelenchoidea. Further cell and molecular evidence are needed to confirm the  
478 integrity of meiosis in *A. besseyi*.

479 To conclude, the availability of the *Aphelenchoides* genome and our comparative  
480 analyses allowed us to pinpoint the major events of horizontal gene transfer in clade IV  
481 nematodes. The results have reinforced the importance of horizontal gene transfers  
482 contributing to multiple adaptations of these nematodes including plant parasitism. In  
483 addition, the various *A. besseyi* genomes will assist in developing molecular diagnostic  
484 tools to distinguish the specific diseases caused by the species complex.

## 485 **Methods**

### 486 **DNA, RNA extraction and sequencing**

487 Nematodes were cultured with *Alternaria citri* on PDA (potato dextrose agar)  
488 medium. All stages of nematodes were collected from the medium, washed with sterile  
489 distilled water, and purified by sucrose gradients. Genomic DNA was extracted using  
490 Qiagen Genomic-tip 100/G according to the manufacturer's instructions, RNA extraction  
491 was conducted using Trizol, and then purified using a lithium chloride purification  
492 method. The DNA paired-end libraries were constructed using either a Nextera DNA  
493 Flex or KAPA hyper library prep kit (Illumina, San Diego, USA); the RNA paired-end  
494 libraries were constructed using a TruSeq Stranded mRNA library prep kit (Illumina, San  
495 Diego, USA). Both DNA and RNA pair-end followed with standard protocol and were  
496 sequenced by Illumina HiSeq 2500 (Illumina, USA) to produce 150-bp paired-end reads.  
497 The HiC library preparation was performed by Phase Genomics (Seattle, WA, USA)  
498 proximo HiC animal protocol with some modification in tissue processing. The enriched  
499 worms were finely chopped by microtube pellet pestle rods for about 2 minutes. The  
500 tissues were crosslinked by adding 1 ml crosslinking solution and incubate for 25  
501 minutes with occasional mixing by rotation. 100 ul quenching solution was added to the  
502 crosslinked tissue and mixed for 20 minutes by rotation. The rest of the preparation  
503 steps follow the protocol. The library was sequenced by Illumina HiSeq 2500 (Illumina,  
504 USA) to produce 150-bp paired-end reads. APFT and AORT were using Pacbio  
505 sequencing system to produce long-read, and the rest of 4 *Aphelenchoides* strains  
506 (APVT, AORJ, *A. bicaudatus*, *A. fujianensis*) were sequenced using the Oxford  
507 Nanopore sequencing platform. The raw nanopore signals were basecalled by Guppy<sup>72</sup>  
508 (ver 0.5.1) producing a total of 5.0-28.4 Gb sequences at least 1 kb in length.

509

### 510 **Assemblies of six *Aphelenchoides* spp.**

511 Raw reads of each species were assembled using Flye (ver 2.8.2)<sup>26</sup> assembler.  
512 The assemblies from Nanopore reads were corrected using Nanopore reads using  
513 Racon<sup>73</sup> (ver 1.4.6) and Medaka<sup>74</sup> (ver 0.10.0). All assemblies were further corrected  
514 using Illumina reads using Pilon<sup>75</sup> (ver 1.22) with five iterations. The *A. pseudobesseyi*  
515 VT assembly was scaffolded using HiC reads and subsequently curated in Juice-box<sup>27</sup>

516 tools. The other five *Aphelenchoides* genomes were reference scaffolded based on this  
517 assembly using Ragtag<sup>76</sup> (ver 1.1).

518

### 519 **Gene prediction and functional annotation**

520 The identification of repetitive elements were computed by RepeatModeler<sup>77</sup> (ver  
521 1.0.8), TransposonPSI (ver 1.0.0; <https://github.com/NBISweden/TransposonPSI>) and  
522 USEARCH<sup>78</sup> (ver 8.1) based on the protocol by Berriman *et al.*<sup>79</sup>. Repeat locations were  
523 then identified by Repeatmasking<sup>80</sup> (ver 4.0.9). RNA-seq reads of six *Aphelenchoides*  
524 strains were trimmed by Trimmomatic<sup>81</sup> (ver 0.36), and aligned to corresponding  
525 assemblies using STAR<sup>82</sup> (ver 2.7.1a). From these mappings, transcripts were inferred  
526 using three approaches: i) assembled based on the mappings as guides using Trinity<sup>83</sup>  
527 (ver 2.84; option: default setting), reconstructed using ii) Stringtie<sup>84</sup> (ver 1.3.4; option:  
528 default setting) and iii) CLASS2<sup>85</sup> (ver 2.17; option: default setting). Transcripts  
529 generated from Trinity were realigned to the reference using GMAP<sup>86</sup> (ver 2017-11-15).  
530 The RNAseq mappings were also used in BRAKER<sup>87</sup> to train species parameter and  
531 generate an initial set of annotations. Proteomes of *Bursaphelenchus xylophilus* and  
532 *Caenorhabditis elegans* were downloaded from Wormbase (WBPS14;  
533 <https://wormbase.org>) and used as homology guides to pick the best transcripts for  
534 each putative locus using MIKADO<sup>88</sup> (ver 1.2.4; option: three Mikado steps, containing  
535 “prepare”, “serialize” and “pick” procedures), and were also used to train MAKER2.  
536 Finally, MAKER2 was invoked to generate a final set of gene annotations using picked  
537 EST evidence and protein evidence from MIKADO transcript and proteomes from  
538 closely related species (*Bursaphelenchus xylophilus* and *Caenorhabditis elegans*), and  
539 used gene models (BUSCO<sup>89</sup>, BRAKER, SNAP<sup>90</sup> and Augustus<sup>91</sup>) as EST hints to train  
540 predicted data with three iterations.

541

### 542 **Comparative analyses**

543 Proteomes of five plant-parasitic nematodes (*Bursaphelenchus xylophilus*,  
544 *Meloidogyne hapla*, *Meloidogyne incognita*, *Globodera pallida*, *Ditylenchus destructor*),  
545 two free-living nematodes (*Caenorhabditis elegans*, *Caenorhabditis briggsae*), six  
546 *Panagrolaimomorpha* (*Propanagrolaimus* sp. JU765, *Panagrellus revidius*,

547 *Panagrolaimus superbus*, *Panagrolaimus* sp. PS1159, *Panagrolaimus davidi* and  
548 *Halicephalobus mephisto*) and one animal parasitic nematode (*Brugia malayi*) were  
549 downloaded from Wormbase<sup>92,93</sup>(ver 14). Orthogroups were determined by  
550 Orthofinder<sup>32</sup> (ver 2.2.7; options: -S diamond). Sequence alignments of each of the  
551 single-copy orthogroups were generated by MAFFT (ver 7.310; options: --maxterate  
552 1000). Then, the concatenated alignment of all single-copy orthogroups was used to  
553 compute a maximum likelihood phylogeny using RAxML<sup>94</sup> (ver 8.2.3; options: -s -T 32 -  
554 N 100 -f a -m PROTGAMMILGF) with 100 bootstrap replicates. Pfam copy numbers of  
555 all 27 nematodes were identified from the results of nematode proteomes blast against  
556 the database of Pfam website (ver 31; <https://pfam.xfam.org/>) using HMMER engine  
557 with e-value smaller than 0.001. Effector enzymes were identified by searching the  
558 nematode proteomes against the CAZyme<sup>95</sup> database (<http://www.cazy.org>) using  
559 HMMER engine with sequence length larger than 80bp. The identified sequence was at  
560 least larger than 0.35 proportion of conserved domain from database and had an e-  
561 value smaller than 1e-15.

562

### 563 **Identification of the HGT genes**

564 The probability of genes having been acquired via HGT was estimated by using  
565 Alieness Index (AI)<sup>45</sup>. Our donor group were generated by non-Metazoans from NCBI  
566 nr database, and the recipient were Metazoans excluding the following species to  
567 prevent self-alignment: Aphelenchoidea, Tylenchida, Rhabditina, Spirurina and  
568 Cephaloboidea. The Alien Index (AI) was estimated by calculating the e-value of  
569 diamond<sup>96</sup> (ver 2.0.14; option: blastx --evalue 0.001) best hits between the donor and  
570 recipient database. Orthogroups having at least one gene with an AI value over 30 were  
571 selected for further analysis. Gains and losses at each node were inferred using Phylip-  
572 Dollop<sup>46</sup> (ver 3.69; options: fdollop -method d -ancseq). Some of the HGT family  
573 acquired branches were manually curated by their evolutionary place of gene phylogeny  
574 due to the fact that nematode genes with AI < 0 were clustered with other HGT genes.  
575 The highest AI value of nematode genes with classified taxonomy hit were chosen to  
576 represent the HGT origin in each orthogroup. Orthogroups with the same CAZyme  
577 annotated and nematode orthology gene AI higher than -50 in those Orthogroups were

578 selected.  $AI < 0$  genes were labelled with “\*”. The orthologs were further combined with  
579 the HGT identified donor sequence from nr database and the specific cellulase  
580 sequence from CAZyme database. To reduce contamination, orthologs of Pfam domain  
581 were annotated and filtered by having at least one major domain (cellulase or pectate  
582 lyase). Sequences of each HGT orthogroup were aligned using MAFFT (options: --  
583 maxiterate 1000 --genafpair) and trimmed by using trimAl<sup>97</sup> (ver 1.4; options: -  
584 gappyout). The ortholog phylogeny were computed by using IQtree<sup>98</sup> (ver 1.6.6; options:  
585 -bb 1000 -alrt 1000). For the CAZyme unclassified HGT orthogroups, the top 2 blast hits  
586 sequences from separated Uniprot (bacteria, fungi, land plants and insect) were used to  
587 confirm the HGT origin.

588

## 589 **AUTHORS CONTRIBUTION**

590 IJT and PJC conceived the study. IJT led the study. YCL, TY and PJC sampled the  
591 *Aphelenchoides* nematodes. YiCL, HMK, WAL conducted the experiments. CKL  
592 analysed the data with input from HHL, YuCL and MRL. IJT and CKL wrote the  
593 manuscript with input from TY, TK, PJC

594

## 595 **DATA AVAILABILITY**

596 The sequencing data and annotation of six *Aphelenchoides* nematodes are publicly  
597 available in NCBI with the BioProject accession PRJNA834627 and scheduled in the  
598 next release WBPS18 of WormBase Parasite. The accession numbers of individual  
599 samples are listed in **supplementary table S2**. The information of Clade IV acquired  
600 HGT orthogroups could be found in github

601 ([https://github.com/lihowfun/CladeIV\\_HGT.git](https://github.com/lihowfun/CladeIV_HGT.git)).

602

## 603 **Funding**

604 This work was supported by Academia Sinica grant (AS-CDA-107-L01) to IJT.

605

## 606 **References**

- 607 1. Blaxter, M. L. *et al.* A molecular evolutionary framework for the phylum Nematoda. *Nat.*  
608 *1998 3926671 392*, 71–75 (1998).
- 609 2. Van Megen, H. *et al.* A phylogenetic tree of nematodes based on about 1200 full-length

- 610 small subunit ribosomal DNA sequences. *Nematology* **11**, 927–950 (2009).
- 611 3. Bird, D. M. K., Jones, J. T., Opperman, C. H., Kikuchi, T. & Danchin, E. G. J. Signatures  
612 of adaptation to plant parasitism in nematode genomes. *Parasitology* **142**, S71 (2015).
- 613 4. Nicol, J. M. *et al.* Current Nematode Threats to World Agriculture. *Genomics Mol. Genet.*  
614 *Plant-Nematode Interact.* 21–43 (2011). doi:10.1007/978-94-007-0434-3\_2
- 615 5. Abad, P. *et al.* Genome sequence of the metazoan plant-parasitic nematode *Meloidogyne*  
616 *incognita*. *Nat. Biotechnol.* 2008 268 **26**, 909–915 (2008).
- 617 6. Kikuchi, T., Cotton, J. A., Dalzell, J. J., Hasegawa, K. & Kanzaki, N. Genomic Insights  
618 into the Origin of Parasitism in the Emerging Plant Pathogen *Bursaphelenchus xylophilus*  
619 Genomic Insights into the Origin of Parasitism in the Emerging Plant Pathogen. (2011).  
620 doi:10.1371/journal.ppat.1002219
- 621 7. Dayi, M. *et al.* Nearly Complete Genome Assembly of the Pinewood Nematode  
622 *Bursaphelenchus xylophilus* Strain Ka4C1. *Microbiol. Resour. Announc.* **9**, (2020).
- 623 8. Cotton, J. A. *et al.* The genome and life-stage specific transcriptomes of *Globodera*  
624 *pallida* elucidate key aspects of plant parasitism by a cyst nematode. *Genome Biol.* 2014  
625 **15**, 1–17 (2014).
- 626 9. Masonbrink, R. *et al.* The genome of the soybean cyst nematode (*Heterodera glycines*)  
627 reveals complex patterns of duplications involved in the evolution of parasitism genes.  
628 *BMC Genomics* **20**, 119 (2019).
- 629 10. Wu, S. *et al.* A reference genome of *bursaphelenchus mucronatus* provides new  
630 resources for revealing its displacement by pinewood nematode. *Genes (Basel)*. **11**,  
631 (2020).
- 632 11. Koutsovoulos, G. D. *et al.* Genome assembly and annotation of *Meloidogyne enterolobii*,  
633 an emerging parthenogenetic root-knot nematode. *Sci. Data* 2020 71 **7**, 1–13 (2020).
- 634 12. Ali, M. A., Azeem, F., Li, H. & Bohlmann, H. Smart parasitic nematodes use multifaceted  
635 strategies to parasitize plants. *Frontiers in Plant Science* (2017).  
636 doi:10.3389/fpls.2017.01699
- 637 13. Danchin, E. G. J., Guzeeva, E. A., Mantelin, S., Berepiki, A. & Jones, J. T. Horizontal  
638 Gene Transfer from Bacteria Has Enabled the Plant-Parasitic Nematode *Globodera*  
639 *pallida* to Feed on Host-Derived Sucrose. *Mol. Biol. Evol.* **33**, 1571–1579 (2016).
- 640 14. Jones, J. T., Furlanetto, C. & Kikuchi, T. Horizontal gene transfer from bacteria and fungi  
641 as a driving force in the evolution of plant parasitism in nematodes. *Nematology* (2005).  
642 doi:10.1163/156854105775142919
- 643 15. Grynberg, P. *et al.* Comparative genomics reveals novel target genes towards specific



- 644 control of plant-parasitic nematodes. (2020). doi:10.20944/preprints202010.0449.v1
- 645 16. Jen, F. Y., Tsay, T. T. & Chen, P. *Aphelenchoides bicaudatus* from ornamental nurseries  
646 in Taiwan and its relationship with some agricultural crops. *Plant Dis.* **96**, 1763–1766  
647 (2012).
- 648 17. Subbotin, S. A. *et al.* The taxonomic status of *Aphelenchoides besseyi* Christie, 1942  
649 (Nematoda: Aphelenchoididae) populations from the southeastern USA, and description  
650 of *Aphelenchoides pseudobesseyi* sp. N. *Nematology* (2020). doi:10.1163/15685411-  
651 bja10048
- 652 18. Oliveira, C. J. *et al.* Morphological and Molecular Identification of Two Florida Populations  
653 of Foliar Nematodes (*Aphelenchoides* spp.) Isolated from Strawberry with the Description  
654 of *Aphelenchoides pseudogoodeyi* sp. N. (Nematoda: Aphelenchoididae) and notes on  
655 their bionomics. *Plant Dis.* **103**, 2825–2842 (2019).
- 656 19. Wang, F. *et al.* Transcriptomic analysis of the rice white tip nematode, *Aphelenchoides*  
657 *besseyi* (Nematoda: Aphelenchoididae). *PLoS One* **9**, (2014).
- 658 20. Lilley, C. J., Kyndt, T. & Gheysen, G. Nematode Resistant GM Crops in Industrialised and  
659 Developing Countries. in *Genomics and Molecular Genetics of Plant-Nematode*  
660 *Interactions* 517–541 (Springer Netherlands, 2011). doi:10.1007/978-94-007-0434-3\_24
- 661 21. Koenning, S. R. *et al.* Survey of crop losses in response to phytoparasitic nematodes in  
662 the United States for 1994. *Journal of Nematology* **31**, 587–618 (1999).
- 663 22. Jones, J. T. *et al.* Top 10 plant-parasitic nematodes in molecular plant pathology. (2013).  
664 doi:10.1111/mpp.12057
- 665 23. Wu, G. L., Kuo, T. H., Tsay, T. T., Tsai, I. J. & Chen, P. J. Glycoside hydrolase (gh) 45  
666 and 5 candidate cellulases in *Aphelenchoides besseyi* isolated from bird's-nest fern.  
667 *PLoS One* **11**, (2016).
- 668 24. Xu, X. *et al.* Population structure and species delimitation of rice white tip nematode,  
669 *Aphelenchoides besseyi* (Nematoda: Aphelenchoididae), in China. *Plant Pathol.* **69**, 159–  
670 167 (2020).
- 671 25. Rybarczyk-Mydlowska, K. *et al.* Small subunit ribosomal DNA-based phylogenetic  
672 analysis of foliar nematodes (*Aphelenchoides* spp.) and their quantitative detection in  
673 complex DNA backgrounds. *Phytopathology* (2012). doi:10.1094/PHYTO-05-12-0114-R
- 674 26. Kolmogorov, M., Yuan, J., Lin, Y. & Pevzner, P. A. Assembly of long, error-prone reads  
675 using repeat graphs. *Nat. Biotechnol.* (2019). doi:10.1038/s41587-019-0072-8
- 676 27. Durand, N. C. *et al.* Juicebox Provides a Visualization System for Hi-C Contact Maps with  
677 Unlimited Zoom. *Cell Syst.* (2016). doi:10.1016/j.cels.2015.07.012

- 678 28. Yoshida, K., Hasegawa, K., Mochiji, N. & Miwa, J. Early Embryogenesis and Anterior-  
679 Posterior Axis Formation in the White-Tip Nematode *Aphelenchoides besseyi*  
680 (Nematoda: Aphelenchoididae). *J. Nematol.* **41**, 17–22 (2009).
- 681 29. Ranallo-Benavidez, T. R., Jaron, K. S. & Schatz, M. C. GenomeScope 2.0 and  
682 Smudgeplots: Reference-free profiling of polyploid genomes. *bioRxiv* 747568 (2019).  
683 doi:10.1101/747568
- 684 30. Cantarel, B. L. *et al.* MAKER: An easy-to-use annotation pipeline designed for emerging  
685 model organism genomes. *Genome Res.* (2008). doi:10.1101/gr.6743907
- 686 31. Finn, R. D. *et al.* Pfam: The protein families database. *Nucleic Acids Research* (2014).  
687 doi:10.1093/nar/gkt1223
- 688 32. Emms, D. M. & Kelly, S. OrthoFinder: phylogenetic orthology inference for comparative  
689 genomics. *Genome Biol.* **20**, 238 (2019).
- 690 33. Kikuchi, T., Eves-Van Den Akker, S. & Jones, J. T. Genome Evolution of Plant-Parasitic  
691 Nematodes. (2017). doi:10.1146/annurev-phyto-080516
- 692 34. Nadachowska-Brzyska, K., Burri, R., Smeds, L. & Ellegren, H. PSMC analysis of effective  
693 population sizes in molecular ecology and its application to black-and-white *Ficedula*  
694 flycatchers. *Mol. Ecol.* **25**, 1058–1072 (2016).
- 695 35. Mitreva, M. *et al.* The draft genome of the parasitic nematode *Trichinella spiralis*. *Nat.*  
696 *Genet.* (2011). doi:10.1038/ng.769
- 697 36. Tcherepanova, I., Bhattacharyya, L., Rubin, C. S. & Freedman, J. H. Aspartic proteases  
698 from the nematode *Caenorhabditis elegans*: Structural organization and developmental  
699 and cell-specific expression of *asp-1*. *J. Biol. Chem.* **275**, 26359–26369 (2000).
- 700 37. McKerrow, J. H. *et al.* *Strongyloides stercoralis*: Identification of a protease that facilitates  
701 penetration of skin by the infective larvae. *Exp. Parasitol.* **70**, 134–143 (1990).
- 702 38. Koch, B. J., Ryan, J. F. & Baxevanis, A. D. The Diversification of the LIM Superclass at  
703 the Base of the Metazoa Increased Subcellular Complexity and Promoted Multicellular  
704 Specialization. doi:10.1371/journal.pone.0033261
- 705 39. Dall, E. & Brandstetter, H. Structure and function of legumain in health and disease.  
706 *Biochimie* **122**, 126–150 (2016).
- 707 40. Holm Viborg, A. *et al.* A subfamily roadmap for functional glyco-genomics of the  
708 evolutionarily diverse Glycoside Hydrolase Family 16 (GH16).  
709 doi:10.1074/jbc.RA119.010619
- 710 41. Coconi Linares, N., Dilokpimol, A., Stålbrand, H., Mäkelä, M. R. & de Vries, R. P.  
711 Recombinant production and characterization of six novel GH27 and GH36  $\alpha$ -

- 712 galactosidases from *Penicillium subrubescens* and their synergism with a commercial  
713 mannanase during the hydrolysis of lignocellulosic biomass. *Bioresour. Technol.* (2020).  
714 doi:10.1016/j.biortech.2019.122258
- 715 42. Shinya, R. *et al.* Possible stochastic sex determination in *Bursaphelenchus* nematodes.  
716 *Nat. Commun.* 2022 131 **13**, 1–14 (2022).
- 717 43. Woodruff, G. C. Patterns of putative gene loss suggest rampant developmental system  
718 drift in nematodes. *bioRxiv* 627620 (2019). doi:10.1101/627620
- 719 44. Danchin, E. G. J. *et al.* Multiple lateral gene transfers and duplications have promoted  
720 plant parasitism ability in nematodes. *Proc. Natl. Acad. Sci. U. S. A.* **107**, 17651–17656  
721 (2010).
- 722 45. Rancurel, C., Legrand, L. & Danchin, E. G. J. Alieness: Rapid detection of candidate  
723 horizontal gene transfers across the tree of life. *Genes (Basel)*. **8**, (2017).
- 724 46. Campoy, E. & González-Martín, A. The Geography as a Regulator of Genetic Flow and  
725 Genetic Structure in Andorra. *Adv. Anthropol.* (2017). doi:10.4236/aa.2017.72008
- 726 47. Morais, M. A. B. *et al.* Two distinct catalytic pathways for GH43 xylanolytic enzymes  
727 unveiled by X-ray and QM/MM simulations. *Nat. Commun.* 2021 121 **12**, 1–13 (2021).
- 728 48. Atanasova, L. *et al.* Evolution and functional characterization of pectate lyase PEL12, a  
729 member of a highly expanded *Clonostachys rosea* polysaccharide lyase 1 family. *BMC*  
730 *Microbiol.* **18**, 1–19 (2018).
- 731 49. PATHOGENICITY OF CURTOBACTERIUM FLACCUMFACIENS pv.  
732 FLACCUMFACIENS TO SEVERAL PLANT SPECIES on JSTOR. Available at:  
733 [https://www.jstor.org/stable/45156052#metadata\\_info\\_tab\\_contents](https://www.jstor.org/stable/45156052#metadata_info_tab_contents). (Accessed: 26th  
734 August 2022)
- 735 50. Kikuchi, T., Jones, J. T., Aikawa, T., Kosaka, H. & Ogura, N. A family of glycosyl  
736 hydrolase family 45 cellulases from the pine wood nematode *Bursaphelenchus*  
737 *xylophilus*. *FEBS Lett.* **572**, 201–205 (2004).
- 738 51. Elling, A. A. *et al.* Sequence mining and transcript profiling to explore cyst nematode  
739 parasitism. *BMC Genomics* **10**, (2009).
- 740 52. Rancurel, C., Legrand, L. & Danchin, E. G. J. Alieness: Rapid detection of candidate  
741 horizontal gene transfers across the tree of life. *Genes (Basel)*. **8**, (2017).
- 742 53. Szitenberg, A. *et al.* Comparative genomics of apomictic root-knot nematodes:  
743 Hybridization, ploidy, and dynamic genome change. *Genome Biol. Evol.* **9**, 2844–2861  
744 (2017).
- 745 54. Schiffer, P. H. *et al.* Signatures of the Evolution of Parthenogenesis and Cryptobiosis in

- 746 the Genomes of Panagrolaimid Nematodes. *iScience* **21**, 587–602 (2019).
- 747 55. Grynberg, P. *et al.* Comparative genomics reveals novel target genes towards specific  
748 control of plant-parasitic nematodes. (2020). doi:10.20944/preprints202010.0449.v1
- 749 56. Holterman, M. *et al.* Disparate gain and loss of parasitic abilities among nematode  
750 lineages. *PLoS One* (2017). doi:10.1371/journal.pone.0185445
- 751 57. Han, Z. *et al.* Horizontally Acquired Cellulases Assist the Expansion of Dietary Range in  
752 *Pristionchus* Nematodes. *Mol. Biol. Evol.* **39**, (2022).
- 753 58. Zheng, J. *et al.* The ditylenchus destructor genome provides new insights into the  
754 evolution of plant parasitic nematodes. *Proc. R. Soc. B Biol. Sci.* (2016).  
755 doi:10.1098/rspb.2016.0942
- 756 59. Wan, X. *et al.* The *Aphelenchus avenae* genome highlights evolutionary adaptation to  
757 desiccation. *Commun. Biol.* **2021 41 4**, 1–8 (2021).
- 758 60. Jagdale, G. B. & Grewal, P. S. Infection behavior and overwintering survival of foliar  
759 nematodes, *Aphelenchoides fragariae*, on *Hosta*. *J. Nematol.* (2006).
- 760 61. Haegeman, A., Jones, J. T. & Danchin, E. G. J. Horizontal Gene Transfer in Nematodes:  
761 A Catalyst for Plant Parasitism? <http://dx.doi.org/10.1094/MPMI-03-11-0055> **24**, 879–887  
762 (2011).
- 763 62. Xia, J. *et al.* Whitefly hijacks a plant detoxification gene that neutralizes plant toxins. *Cell*  
764 (2021). doi:10.1016/j.cell.2021.02.014
- 765 63. Brown, A. M. V. *et al.* Comparative genomics of wolbachia-cardinium dual endosymbiosis  
766 in a plant-parasitic nematode. *Front. Microbiol.* **9**, 2482 (2018).
- 767 64. Holterman, M., Schratzberger, M. & Helder, J. Nematodes as evolutionary commuters  
768 between marine, freshwater and terrestrial habitats. *Biol. J. Linn. Soc.* **128**, 756–767  
769 (2019).
- 770 65. Ma, J. *et al.* Major episodes of horizontal gene transfer drove the evolution of land plants.  
771 *Mol. Plant* **15**, 857–871 (2022).
- 772 66. Li, Y. *et al.* HGT is widespread in insects and contributes to male courtship in  
773 lepidopterans. *Cell* **185**, 2975–2987.e10 (2022).
- 774 67. Ren, L., Huang, W., Cannon, E. K. S., Bertioli, D. J. & Cannon, S. B. A mechanism for  
775 genome size reduction following genomic rearrangements. *Front. Genet.* (2018).  
776 doi:10.3389/fgene.2018.00454
- 777 68. Cicconardi, F. *et al.* Chromosome Fusion Affects Genetic Diversity and Evolutionary  
778 Turnover of Functional Loci but Consistently Depends on Chromosome Size. *Mol. Biol.*  
779 *Evol.* **38**, 4449–4462 (2021).

- 780 69. Wang, J. *et al.* Comparative genome analysis of programmed DNA elimination in  
781 nematodes. *Genome Res.* **27**, 2001–2014 (2017).
- 782 70. Fradin, H. *et al.* Genome Architecture and Evolution of a Unichromosomal Asexual  
783 Nematode. *Curr. Biol.* **27**, 2928–2939.e6 (2017).
- 784 71. Yin, D. *et al.* Rapid genome shrinkage in a self-fertile nematode reveals sperm  
785 competition proteins. *Science (80-. )*. **359**, 55–61 (2018).
- 786 72. Wick, R. R., Judd, L. M. & Holt, K. E. Performance of neural network basecalling tools for  
787 Oxford Nanopore sequencing. *Genome Biol.* (2019). doi:10.1186/s13059-019-1727-y
- 788 73. Vaser, R., Sović, I., Nagarajan, N. & Šikić, M. Fast and accurate de novo genome  
789 assembly from long uncorrected reads. *Genome Res.* (2017). doi:10.1101/gr.214270.116
- 790 74. Medaka: Sequence correction by using ONT research.  
791 <https://github.com/nanoporetech/medaka>
- 792 75. Walker, B. J. *et al.* Pilon: An integrated tool for comprehensive microbial variant detection  
793 and genome assembly improvement. *PLoS One* (2014).  
794 doi:10.1371/journal.pone.0112963
- 795 76. Alonge, M. *et al.* RaGOO: Fast and accurate reference-guided scaffolding of draft  
796 genomes. *Genome Biol.* **20**, 224 (2019).
- 797 77. Flynn, J. M. *et al.* RepeatModeler2 for automated genomic discovery of transposable  
798 element families. *Proc. Natl. Acad. Sci. U. S. A.* (2020). doi:10.1073/pnas.1921046117
- 799 78. Edgar, R. C. & Bateman, A. Search and clustering orders of magnitude faster than  
800 BLAST. *Bioinformatics* **26**, 2460–2461 (2010).
- 801 79. Coghlan, A., Coghlan, A., Tsai, I. J. & Berriman, M. Creation of a comprehensive repeat  
802 library for a newly sequenced parasitic worm genome. *Protoc. Exch.* (2018).  
803 doi:10.1038/protex.2018.054
- 804 80. Tarailo-Graovac, M. & Chen, N. Using RepeatMasker to identify repetitive elements in  
805 genomic sequences. *Current Protocols in Bioinformatics* (2009).  
806 doi:10.1002/0471250953.bi0410s25
- 807 81. Bolger, A. M., Lohse, M. & Usadel, B. Trimmomatic: A flexible trimmer for Illumina  
808 sequence data. *Bioinformatics* (2014). doi:10.1093/bioinformatics/btu170
- 809 82. Dobin, A. & Gingeras, T. R. Mapping RNA-seq Reads with STAR. *Curr. Protoc.*  
810 *Bioinforma.* (2015). doi:10.1002/0471250953.bi1114s51
- 811 83. Grabherr, M. G. *et al.* Full-length transcriptome assembly from RNA-Seq data without a  
812 reference genome. *Nat. Biotechnol.* (2011). doi:10.1038/nbt.1883
- 813 84. Pertea, M. *et al.* StringTie enables improved reconstruction of a transcriptome from RNA-

- 814 seq reads. *Nat. Biotechnol.* (2015). doi:10.1038/nbt.3122
- 815 85. Song, L., Sabunciyan, S. & Florea, L. CLASS2: Accurate and efficient splice variant  
816 annotation from RNA-seq reads. *Nucleic Acids Res.* (2016). doi:10.1093/nar/gkw158
- 817 86. Wu, T. D. & Watanabe, C. K. GMAP: A genomic mapping and alignment program for  
818 mRNA and EST sequences. *Bioinformatics* (2005). doi:10.1093/bioinformatics/bti310
- 819 87. Hoff, K. J., Lange, S., Lomsadze, A., Borodovsky, M. & Stanke, M. BRAKER1:  
820 Unsupervised RNA-Seq-based genome annotation with GeneMark-ET and AUGUSTUS.  
821 *Bioinformatics* (2016). doi:10.1093/bioinformatics/btv661
- 822 88. Venturini, L., Caim, S., Kaithakottil, G. G., Mapleson, D. L. & Swarbreck, D. Leveraging  
823 multiple transcriptome assembly methods for improved gene structure annotation.  
824 *Gigascience* **7**, (2018).
- 825 89. Simão, F. A., Waterhouse, R. M., Ioannidis, P., Kriventseva, E. V. & Zdobnov, E. M.  
826 BUSCO: Assessing genome assembly and annotation completeness with single-copy  
827 orthologs. *Bioinformatics* (2015). doi:10.1093/bioinformatics/btv351
- 828 90. Korf, I. Gene finding in novel genomes. *BMC Bioinformatics* **5**, 1–9 (2004).
- 829 91. Stanke, M. *et al.* AUGUSTUS: A b initio prediction of alternative transcripts. *Nucleic Acids*  
830 *Res.* (2006). doi:10.1093/nar/gkl200
- 831 92. Howe, K. L., Bolt, B. J., Shafie, M., Kersey, P. & Berriman, M. WormBase ParaSite – a  
832 comprehensive resource for helminth genomics. *Mol. Biochem. Parasitol.* **215**, 2 (2017).
- 833 93. Davis, P. *et al.* WormBase in 2022—data, processes, and tools for analyzing  
834 *Caenorhabditis elegans*. *Genetics* **220**, (2022).
- 835 94. Stamatakis, A. RAxML version 8: A tool for phylogenetic analysis and post-analysis of  
836 large phylogenies. *Bioinformatics* (2014). doi:10.1093/bioinformatics/btu033
- 837 95. Xu, J. -H. Carbohydrate Active Enzyme database. in *Catalysis from A to Z* (2020).  
838 doi:10.1002/9783527809080.cataz02801
- 839 96. Buchfink, B., Xie, C. & Huson, D. H. Fast and sensitive protein alignment using  
840 DIAMOND. *Nature Methods* (2014). doi:10.1038/nmeth.3176
- 841 97. Capella-Gutiérrez, S., Silla-Martínez, J. M. & Gabaldón, T. trimAl: A tool for automated  
842 alignment trimming in large-scale phylogenetic analyses. *Bioinformatics* (2009).  
843 doi:10.1093/bioinformatics/btp348
- 844 98. Nguyen, L. T., Schmidt, H. A., Von Haeseler, A. & Minh, B. Q. IQ-TREE: A fast and  
845 effective stochastic algorithm for estimating maximum-likelihood phylogenies. *Mol. Biol.*  
846 *Evol.* (2015). doi:10.1093/molbev/msu300
- 847